Electronic Supporting Information

Tuning the electrochemical performance of covalent organic framework cathodes for Li- and Mg-based batteries: the influence of electrolyte and binder

Olivera Lužanin,[a,b] Raquel Dantas,[c] Robert Dominko,[a,b,d] Jan Bitenc*[a,b] and Manuel Souto*[c]

[a] National Institute of Chemistry, Hajdrihova 19, 1000, Ljubljana, Slovenia

[b] Faculty of Chemistry and Chemical Technology, University of Ljubljana, Večna pot 113, 1000, Ljubljana, Slovenia. e-mail: jan.bitenc@ki.si

[c] Department of Chemistry, CICECO-Aveiro Institute of Materials, University of Aveiro, Aveiro, 3810-393, Portugal. e-mail: manuel.souto@ua.pt

[d] Alistore-European Research Institute, CNRS FR 3104, Hub de l'Energie, Rue Baudelocque, 80039, Amiens, France

Contents

Table S1. Summary of electrolytes, binders, electrode composition and practical capacity of reported COF-based cathode materials for lithium batteries.

COF-based cathode material	Electrolyte	Binder	Electrode composition (COF/CB/ Binder)	Practical capacity (mAh/g) and current density used (C or A/g)
D_{TP}-A_{NDI}-COF@CNTs [1]	$LiPF_6$ in EC/DMC (1:1) (1 M)	PVdF	7/2/2	74 mAh/g at 2.4 C
Tp–DANT-COF [2] Tb–DANT-COF [2]	$LiPF_6$ in EC/DMC (1:1) (1 M)	PVdF	6/2/2	104 mAh/g at 0.37 C 144 mAh/g at 0.34 C
DAAQ-TFP-COF [3] DAAQ-ECOF [3] DABQ-TFP-ECOF [3] TEMPO-ECOF [3]	LiTFSI in TEGDME (1 M)	PVdF	6/3/1	110 mAh/g at 0.02 A/g 145 mAh/g at 0.02 A/g 210 mAh/g at 0.02 A/g 115 mAh/g at 0.02 A/g
PIBN-G [4]	LiTFSI in DOL/DME (1 M)	PVdF	8/1/1	271 mAh/g at 0.1 C
CCP-HATN [5] CCP-HATN@CNT [5]	LiTFSI in DOL/DME (1 M)	Sodium alginate	8/1/1	62.5 mAh/g at 0.1 A/g 116 mAh/g at 0.1 A/g
PI-COF [6] PI-ECOF-1 [6] PI-ECOF-2 [6]	$LiPF_6$ in DMC/EC/EMC (1:1:1) LiTFSI in DOL/DME (1:1) (1 M)	PVdF	6/3/1	85 mAh/g at 0.1 C 112 mAh/g at 0.1 C 103 mAh/g at 0.1 C
2D-PAI@CNT [7]	LiTFSI in DOL/DME (1:1) (1 M)	Sodium alginate	8/1/1	104.4 mAh/g at 0.1 A/g
PPTODB@MWCNT [8]	$LiPF_6$ in EC/DMC (1:1) (1 M)	-	7/3	198 mAh/g at 0.02 A/g
DAAQ-TFP-COF, DAPH-TFP-COF, PEDOT@ DAAQ-TFP-COF, PEDOT@ DAPH-TFP-COF, [9]	$LiPF_6$ in EC/DMC (1:1) (1 M)	PVdF	6/3/1	53.5 mAh/g at 0.5 C 81.7 mAh/g at 0.5 C 59.8 mAh/g at 0.5 C 93.2 mAh/g at 0.5 C
COF-TRO [10]	Argyrodite (SE)	-	5/4/1	268 mAh/g at 0.1 C
DAPO-TpOMe-COF [11]	$LiPF_6$ in EC/DMC (1:1) (1 M)	PVdF	6/3/1	68 mAh/g at 0.1 A/g
AZO-1@CNTs [12] AZO-2@CNTs [12] AZO-3@CNTs [12]	LiTFSI in DOL/DME (1:1) (1 M)	PVdF	7/2/1	140 mAh/g at 0.5 C (0.06 A/g) 60 mAh/g at 1 C (0.12 A/g) 50 mAh/g at 1 C (0.12 A/g)
TAPB-NDI COF [13]	$LiPF_6$ in EC/PC/DMC (1:1:3) (0.7 M)	PVdF	6/2.5/1.5	33 mAh/g at 0.03 A/g
E-TP-COF [14]	LiTFSI in DOL/DME (1:1) (1 M)	PVdF	6/3/1	110 mAh/g at 0.2 A/g
Azo-CTF [15]	LiTFSI in DOL/DME (1:1) (1 M)	PVdF	6/2.5/1.5	205 mAh/g at 0.1 A/g
PT-COF50 [16] PT-COF10 [16] PT-COF [16]	LiTFSI in DOL/DME (1:1) (1 M)	PVdF	6/3/1	280 mAh/g at 0.2 A/g 225.0 mAh/g at 0.2 A/g 193.0 mAh/g at 0.2 A/g
HATN-AQ-COF [17]	LiTFSI in DOL/DME (1:1) (1 M)	PVdF	5/4/1	319 mAh/g at 0.5 C (0.18 A/g)
Be-PICOF [18] Na-PICOF [18] Pe-PICOF [18]	LiTFSI in DOL/DME (1:1) (1 M)	PVdF	2/7/1	114 mAh/g at 0.05 A/g 102 mAh/g at 0.05 A/g 91 mAh/g at 0.05 A/g

TPPDA-PICOF [19]	$LiPF_6$ in EC/DMC (1:1) (1 M)	PVdF	5/4/1	47 mAh/g at 0.2 A/g
TP-TA COF [20]	$LiPF_6$ in EC/EMC (3:7) (1 M)	PVdF	8/1/1	207 mAh/g at 0.2 A/g
HATN-HHTP@CNT [21]	LiTFSI in DOL/DME (1:1) (1 M)	Sodium alginate	8/1/1	230 mAh/g at 0.05 A/g
PhDBP-TFP COF [22] DBP-Ph-TFP POP [22]	$LiPF_6$ in EC/DMC (1:1) (1 M)	PVdF	3/5/2	26 mAh/g at 0.1 A/g 14 mAh/g at 0.1 A/g
TFPPy-ICTO-COF [23] TFPPer-ICTO-COF [23]	$LiPF_6$ in EC/DMC (1:1) (1 M)	lithium polyacrylate	7/2/1	338 mAh/g at 0.1 A/g 303 mAh/g at 0.1 A/g

1. General methods and materials

All reagents and solvents were of high purity grade and were purchased from Sigma-Aldrich Co., TCI, and ChemExtension Co., Ltd. Powder X-Ray Diffraction (PXRD) data were collected at ambient temperature on an Empyrean PANalytical diffractometer, with a working wavelength of λ_1 = 1.540598 Å and λ_2 = 1.544426 Å (Cu K$\alpha_{1,2}$ X-radiation), equipped with a PIXcel 1D detector, a capillary sample holder, and an Incident beam PreFIX module with elliptical X-ray mirror for Cu radiation (45 kV, 40 mA). Infrared (IR) spectra were recorded in an ATR FTIR GALAXY SERIES FT-IR 7000 (Mattson Instruments) spectrometer in the 4000-400 cm^{-1} range using powdered samples. Thermogravimetric analysis (TGA) was carried out with a Shimadzu TGA 50 equipment in the 25-600 ºC temperature range under a 5 ºC min^{-1} scan rate and a N_2 flow of 20 $mL \cdot min^{-1}$. N_2 adsorption isotherms were measured using a Micromeritics ASAP2020 volumetric instrument under static adsorption conditions. Before measurement, samples were heated at 323 K overnight and outgassed to 10^{-6} Torr. Brunauer-Emmet-Teller (BET) and Langmuir analyses were carried out to determine the total specific surface areas from the N_2 isotherms at 77 K. SEM images were acquired on a Hitachi S4100 field emission gun tungsten filament instrument working at 25 kV and on a high-resolution Hitachi SU-70 working at 4 kV. Samples were prepared by deposition on aluminium sample holders followed by carbon coating using an Emitech K950X carbon evaporator. The electrochemical experiments were performed on an Autolab electrochemical workstation (PGSTAT302N with FRA32M Module) connected to a personal computer that uses Nova 2.1 electrochemical software. A typical three-electrode experimental cell equipped with a glassy carbon as working electrode, platinum wire as the counter electrode, and Ag/AgCl as the pseudoreference electrode was used for the electrochemical characterization. The electrochemical properties were studied measuring CV under inert (N_2) atmosphere at different scan rates in previously N_2-purged 0.1 M $TBAPF_6/CH_2Cl_2$ solutions. Ferrocene was added as an internal standard upon completion of each experiment.

2. Synthesis and characterization of DAAQ-TFP-COF

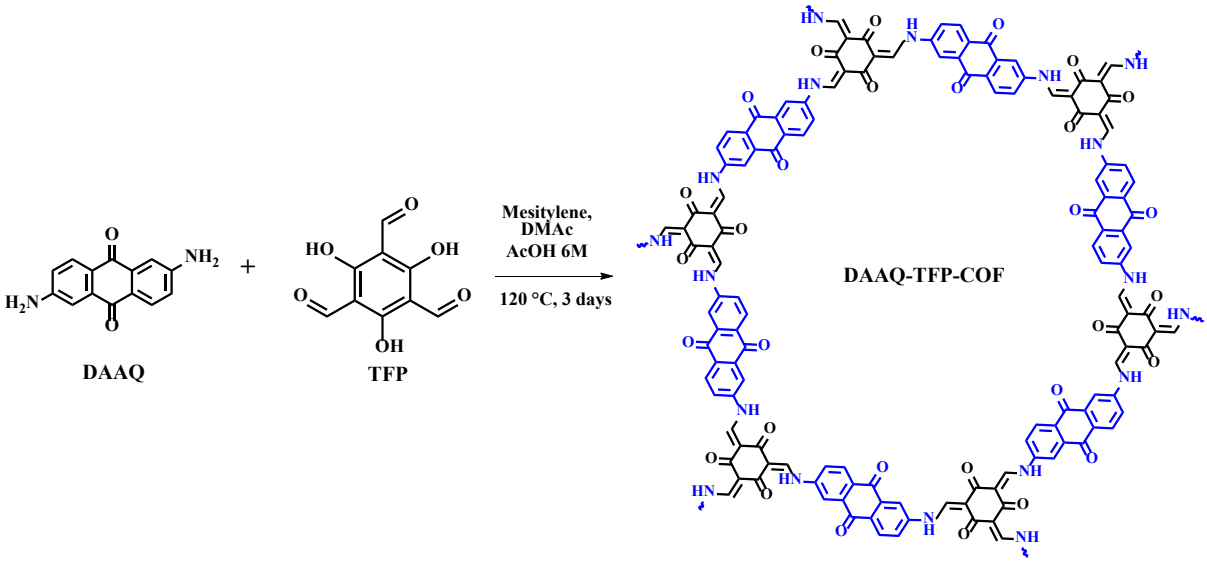

Scheme S1. Synthesis of **DAAQ-TFP-COF**.

DAAQ-TFP-COF was synthesized according to a reported procedure. [24] First, 1,3,5-triformylphloroglucinol (TFP) (20.0 mg, 0.095 mmol), and 2,6-diaminoanthraquinone (DAAQ) (34.0 mg, 0.14 mmol), dimethylacetamide (0.9 ml) and mesitylene (0.3 mL) were added into a Pyrex 4-mL vial and the suspension was sonicated at room temperature for five minutes. Then, aqueous acetic acid 6 M (50 µL) was added to the vial and the suspension was sonicated again for a few minutes. The vial was then tightly sealed and heated at 120 ºC for 3 days. Afterwards, the reaction mixture was cooled to room temperature and the precipitate was filtrated and exhaustively washed with *N*,*N*-dimethylformamide (DMF) and acetone. The material was then dried at 120°C overnight resulting in a dark red powder (42 mg; 85% yield).

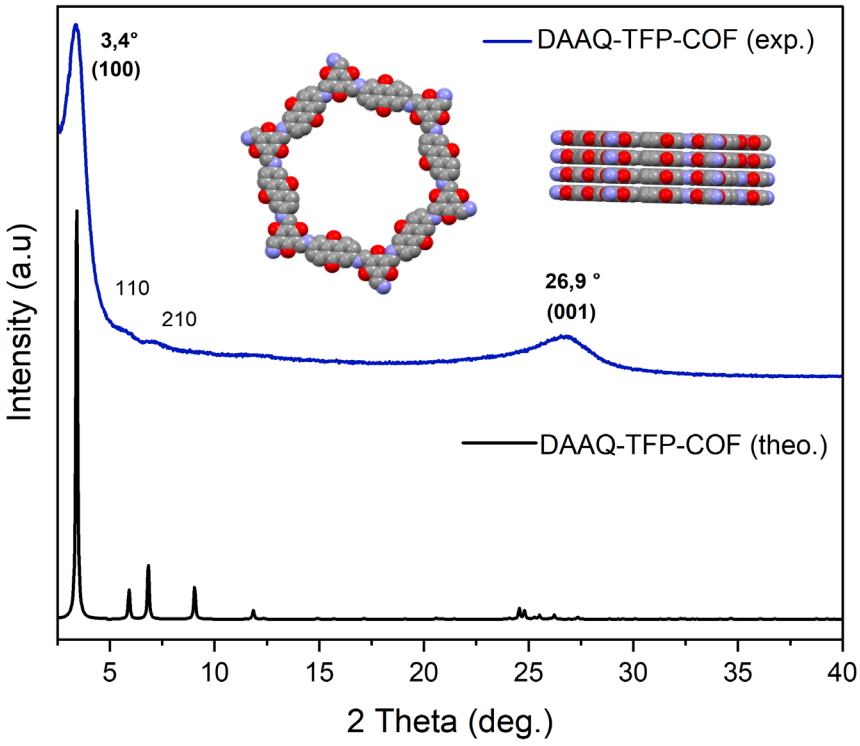

Figure S1. Powder X-ray diffraction (PXRD) pattern of **DAAQ-TFP-COF** (experimental and simulated). The inset shows top and lateral views of the COF model.

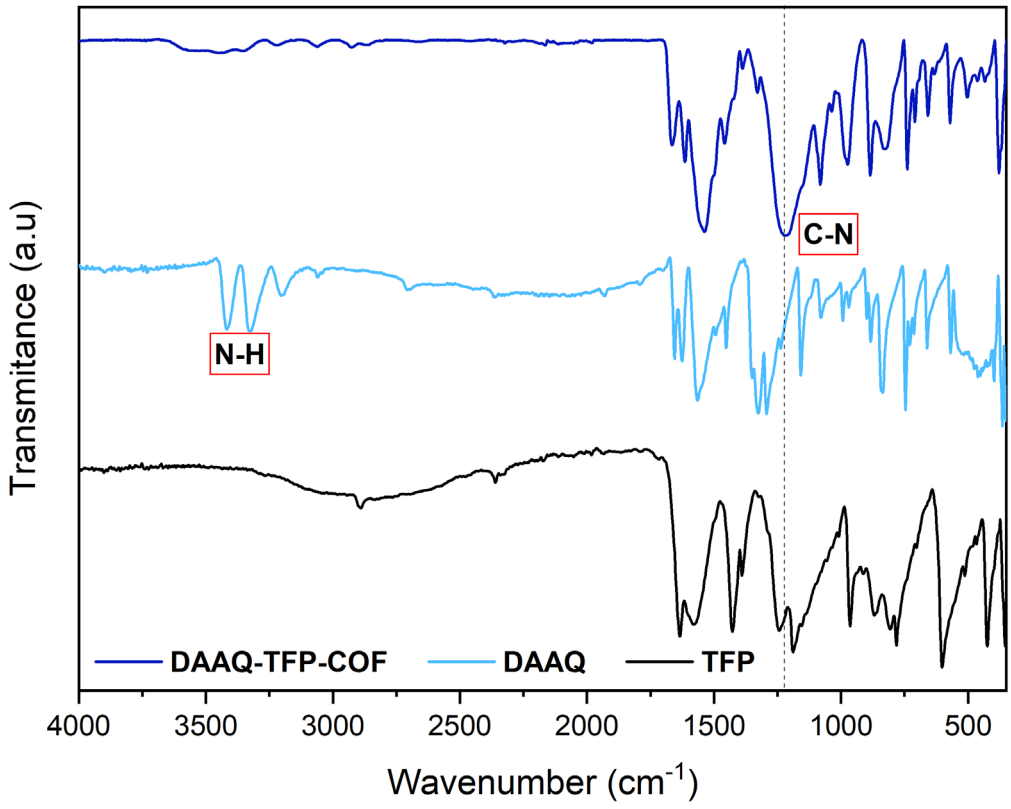

Figure S2. IR spectra of **DAAQ-TFP-COF** and precursors (DAAQ and TFP).

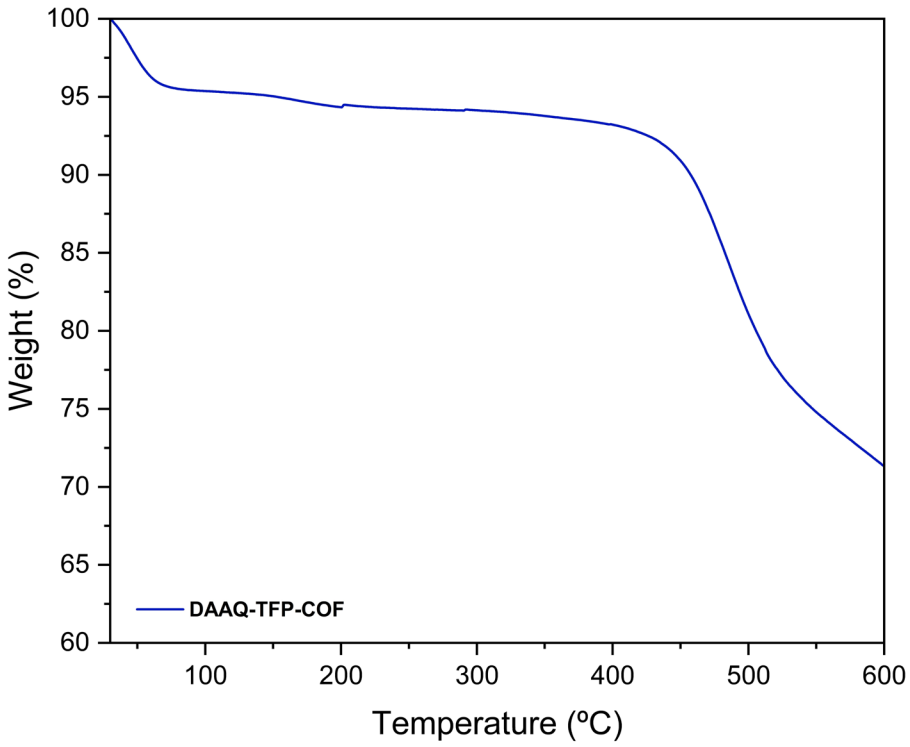

Figure S3. Thermogravimetric analysis (TGA) of as-synthesized **DAAQ-TFP-COF** in the 25-600 ºC temperature range under a 5 ºC min^{-1} scan rate and a N_2 flow of 20 $mL \cdot min^{-1}$.

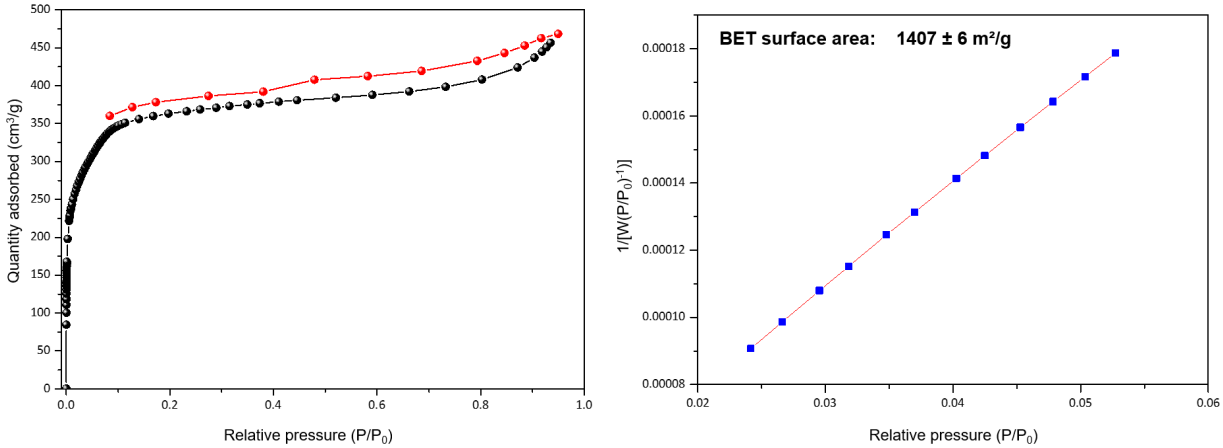

Figure S4. N_2 adsorption (black circles) and desorption (red circles) isotherms of **DAAQ-TFP-COF** at 77 K and BET analysis.

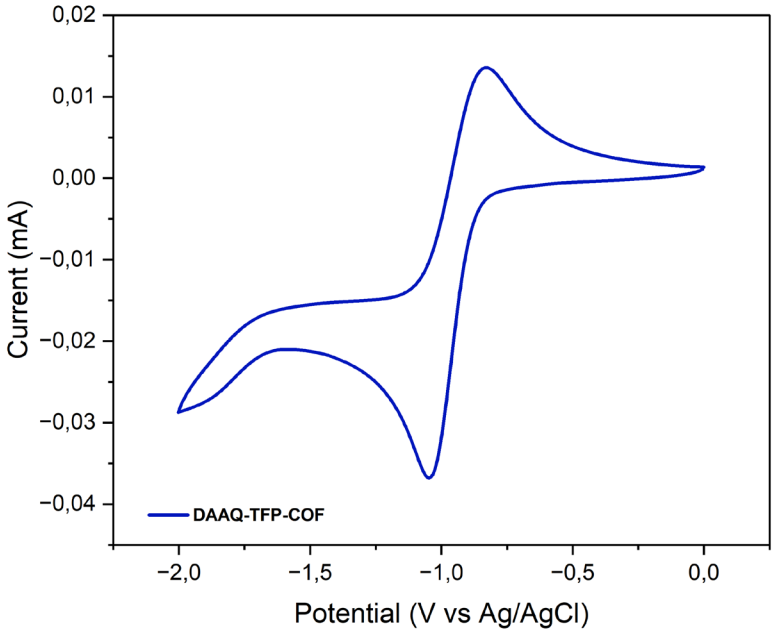

Figure S5. Solid-state cyclic voltammetry (CV) of **DAAQ-TFP-COF** in CH_3CN using $TBAPF_6$ 0.1 M as the electrolyte at 0.1 V s^{-1} scan rate. A platinum wire was used as the counter electrode, and Ag/AgCl as the pseudo-reference electrode. Ferrocene was added as an internal standard. All potentials are quoted versus Ag/AgCl.

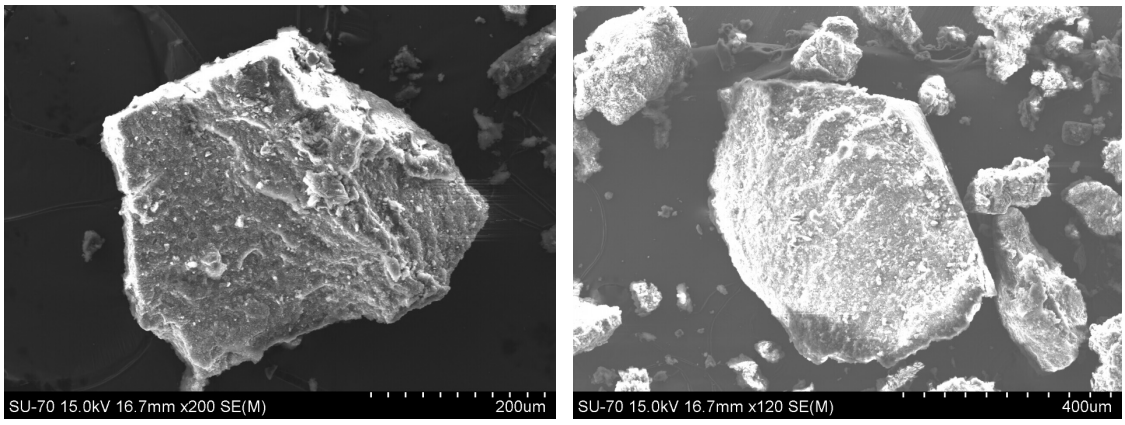

Figure S6. SEM images of **DAAQ-TFP-COF**.

3. Electrode preparation

1) PVdF electrodes: Electrodes were prepared by mixing active material, carbon black (Printex XE-2), and PVdF in NMP. After milling under the same condition as with PTFE-containing composite, the slurry was casted on carbon-coated Al foil, using a doctor blade. After drying in vacuum for 24 h at 80 ºC, electrodes were cut (12 mm) and dried overnight at 50 ºC before they were transferred inside the glovebox. Mass loading of the electrodes was between 0.8-1.8 mg cm^{-2}.

2) PTFE electrodes: Electrodes were prepared by mixing active material, carbon black (Printex XE-2), and PTFE in weight ratio 6:3:1. All of the components were mixed in a stainless-steel ball-milling jar in the dispersion of isopropanol (Retsch PM100 at 300 rpm for 30 minutes). A black, gum-like compound was obtained and then mixed in mortar and pestle with additional isopropanol. Afterward, gum was rolled between the glass plate and parchment paper. Self-standing 12 mm electrodes were cut. After 12 h drying at 50 ºC, electrodes were pressed onto carbon-coated aluminum current collector (0.9 t per cm^2, 30 s). Electrodes were then dried again at 50 ºC overnight and then transferred inside an Ar-filled glovebox. Mass loading of the electrodes ranged between 1.5-2.5 mg cm^{-2}.

4. Electrolyte preparation

1,2-dimethoxyethane (DME) (Sigma-Aldrich, HPLC grade, 99.9%), 1,3-dioxolane (DOL) (Acros, 99.8%), and tetraethylene glycol dimethyl ether (TEGDME) (Acros, 99.8%) were dried with 4 Å molecular sieves for several days, refluxed with Na/K alloy (ca. 1 mL l^{-1}), and then fractionally distilled. γ-butyrolactone is not compatible with Na/K alloy. Hence, it was dried several times with molecular sieves and fractionally distilled (Merck, 99.8%) The final water content in distilled solvents was below 1 ppm as determined by Karl-Fischer titration.
LiTFSI (Silgma-Aldrich, 99.95%) was dried overnight at 120 °C under vacuum before transfer to the glovebox. Lithium perchlorate (Sigma Aldrich, battery grade) and $LiPF_6$ in EC/DEC (E-lyte Innovations) were used as received. All the glassware was dried at 80 ºC prior to use. All of the electrolyte preparation and handling were performed inside an Ar-filled glovebox with H_2O and O_2 content below 0.5 ppm.

Prepared electrolytes:
1 M LiTFSI in DOL/DME (50:50, vol%)
1 M LiTFSI in TEGDME
1 M $LiPF_6$ in EC/DEC (50:50, vol%)
1 M $LiClO_4$ in GBL

To assess any potential dissolution issues of active material, electrodes were soaked in 1 mL of each electrolyte for 48 h. As the photos below show, the active material is stable in all of the selected electrolytes, with no apparent dissolution occurring after two days of soaking.

Figure S7. Electrodes containing PTFE binder soaked for 48 h in electrolytes. No apparent dissolution of the active material was observed.

5. Electrochemical cell setups

Half-cell setup: Half-cell testing was performed in two-electrode Swagelok cells. The working electrode was either PTFE or PVdF COF (12 mm), prepared through the previously described procedure. Two separators were used per cell, one glassy fiber (Whatman, 260 μm, 13 mm) and one Celgard 2320 (13 mm). Separators were soaked in 65 μl of the electrolyte of choice. The counter/reference electrode was Li foil (110 μm, FMC), rolled to a fine shine and cut into a 12 mm disc. The current collector on the Li side was stainless steel disc.

Symmetric cell setup: Symmetric cells were assembled by combining two DAAQ-TFP-COF electrodes, one in fully charged and other in fully discharged state. Electrode in discharged state was discharged with the current of 50 mA g^{-1} down to 1.5 V followed by a 12 h voltage hold. Fully charged electrode was used as-prepared, without any electrochemical preconditioning. One GF/A soaked with 90 μl of electrolyte was used as a separator.

6. Electrochemical tests

All of the galvanostatic electrochemical experiments were performed using VMP3 Bio-Logic potentiostat/galvanostat controlled by EC-Lab® software. All of the cells were assembled inside an Ar-filled glovebox. Galvanostatic cycling on half-cells was done in the potential window from 1.5 to 3.5 V. Stability over 100 cycles in different electrolytes was performed at the current density of 150 mA g^{-1}. All of the electrochemical tests were performed at room temperature.

- PVdF-based electrodes

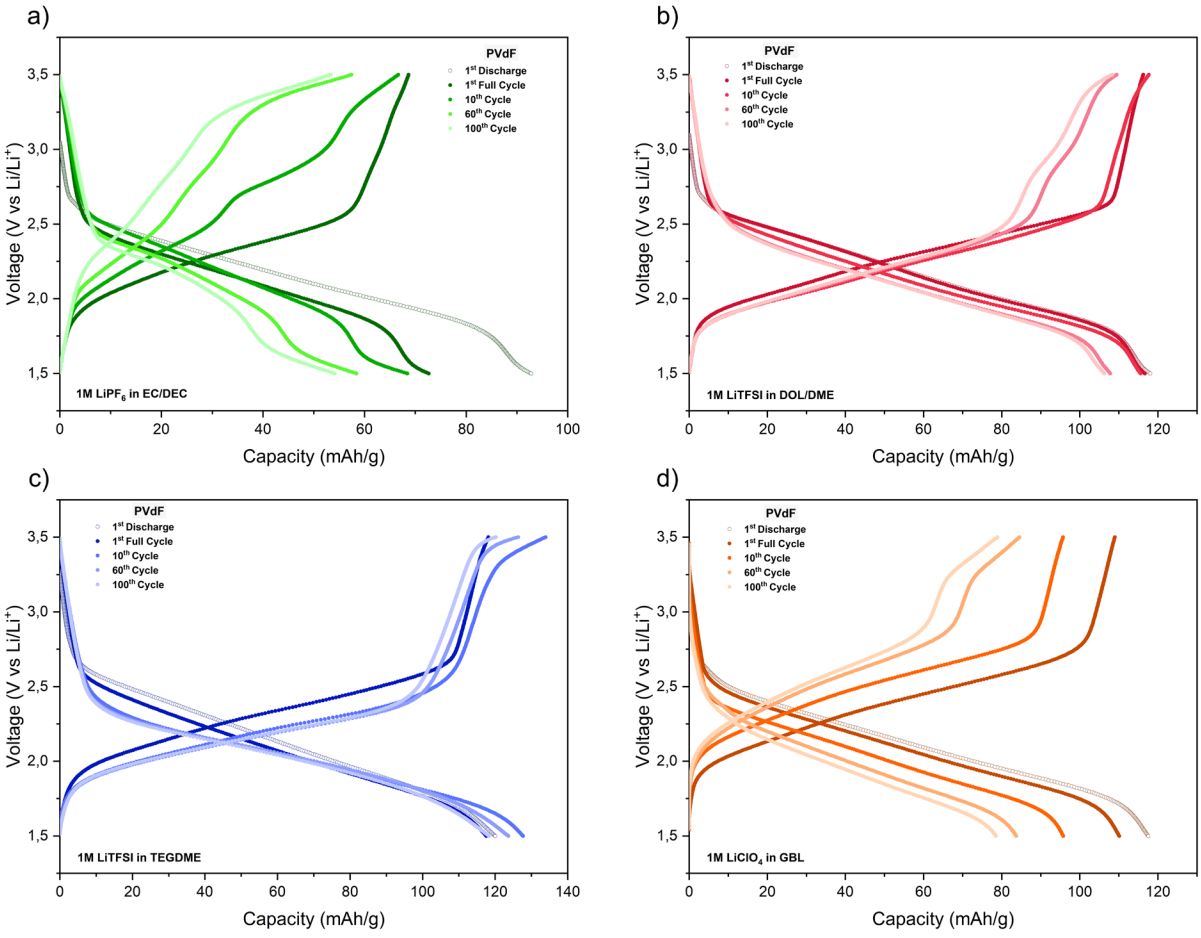

Figure S8. Galvanostatic profiles of DAAQ-TFP-COF electrodes in different electrolytes: (a) 1 M $LiPF_6$ in EC/DEC, (b) 1 M LiTFSI in DOL/DME, (c) 1 M LiTFSI in TEGDME, (d) 1 M $LiClO_4$ in GBL. PVdF was used as a binder and the current density was 150 mA g^{-1}.

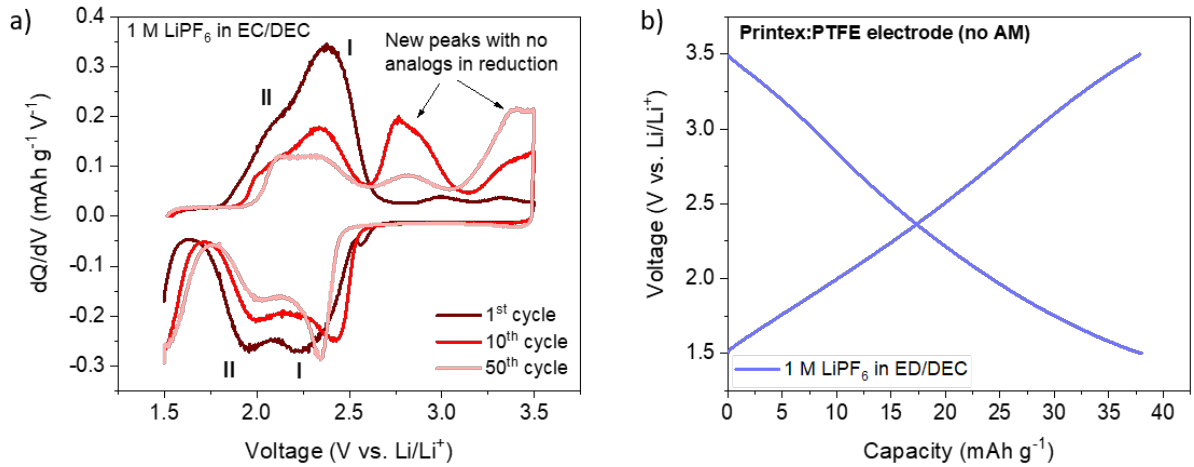

Figure S9. a) Derivative curves of DAAQ-TFP-COF in 1 M $LiPF_6$ EC/DEC obtained at 50 mA g^{-1} obtained in 1st, 10th, and 50th cycle. b) Galvanostatic profile of electrode containing only carbon black and PTFE obtained in 1 M $LiPF_6$ in EC/DEC obtained at 20 mA g^{-1}.

- **PTFE-based electrodes**

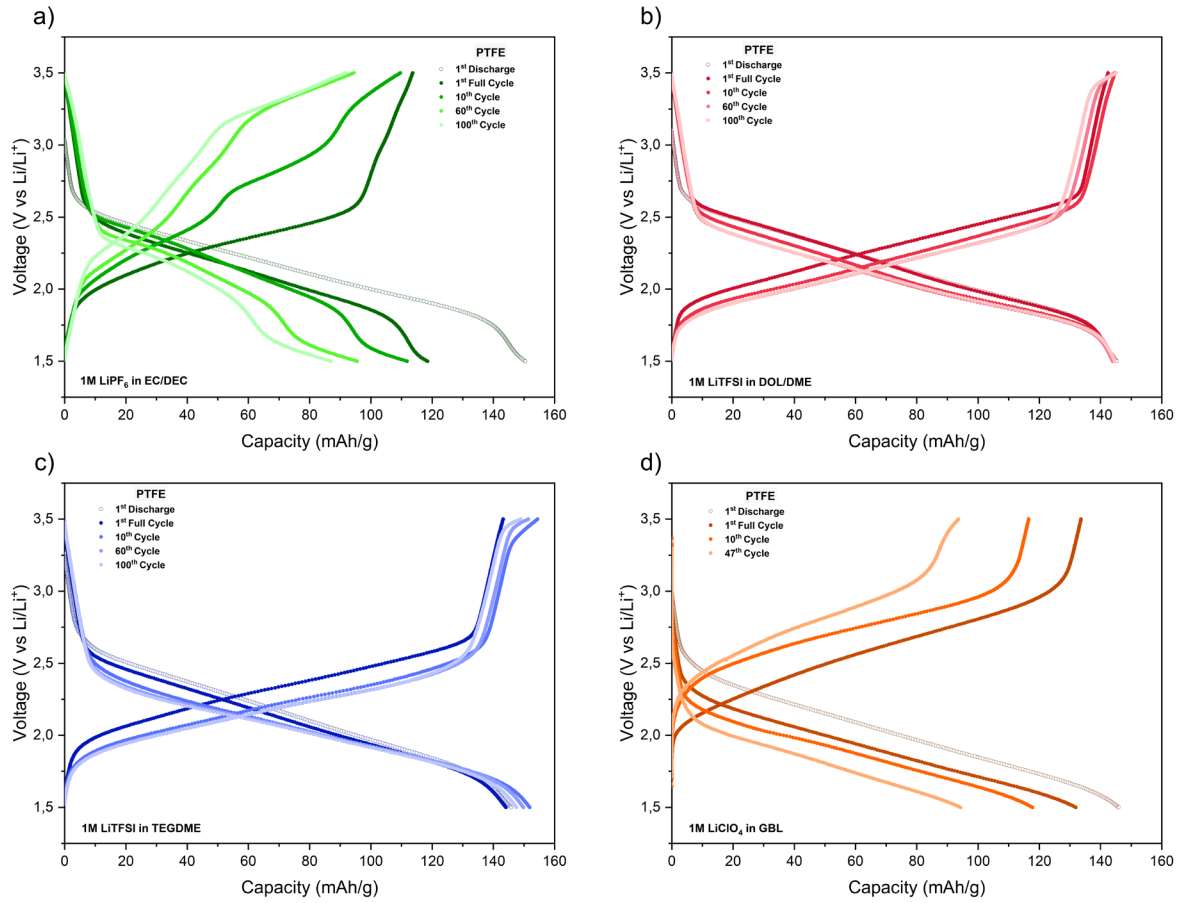

Figure S10. Galvanostatic profiles of DAAQ-TFP-COF electrodes in different electrolytes: (a) 1 M $LiPF_6$ in EC/DEC, (b) 1 M LiTFSI in DOL/DME, (c) 1 M LiTFSI in TEGDME, (d) 1 M $LiClO_4$ in GBL. PTFE was used as a binder and the current density was 150 mA g^{-1}. The inset shows photos of glassy fibre separators after 100 cycles.

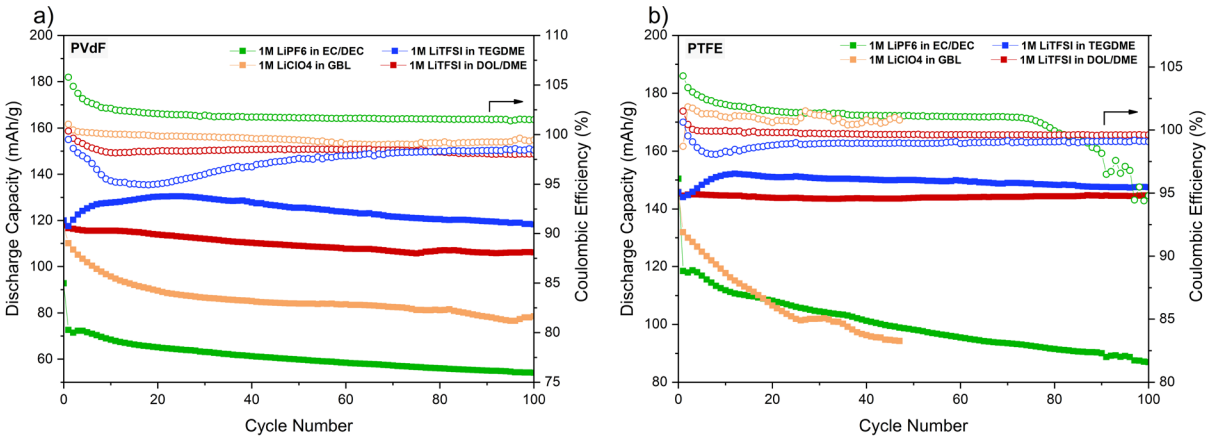

Figure S11. Stability and Coulombic efficiencies of DAAQ-TFP-COF electrodes with PVdF (a) and PTFE (b) in 1 M $LiPF_6$ in EC/DEC (green), 1 M LiTFSI in DOL/DME (red), 1 M LiTFSI in TEGDME (blue), and 1 M $LiClO_4$ in GBL (orange).

Table S2. Initial discharge capacity and capacity retention after 100 cycles in four different electrolytes at the current density of 150 mA g^{-1}. The first row for each electrolyte represents PVdF electrode (lighter shade) and the second row PTFE electrode (darker shade).

Electrolyte	Binder	Initial Capacity (mAh g^{-1})	Capacity at Cycle 100 (mAh g^{-1})	Capacity Retention at Cycle 100 (%)
1M $LiPF_6$ in EC/DEC	PVdF	92,8	54,1	58%
	PTFE	150,5	87,0	58%
1M LiTFSI in DOL/DME	PVdF	118,0	106,2	90%
	PTFE	145,3	144,7	100%
1M LiTFSI in TEGDME	PVdF	120,0	118,3	99%
	PTFE	145,8	147,5	101%
1M $LiClO_4$ in GBL	PVdF	117,5	78,5	67%
	PTFE	145,9	94,3*	65%*

*** After 47 cycles instead of 100, due to repeated cell failure**

7. Scanning Electron Microscopy (SEM)

SEM imaging was performed FE-SEM Supra 35 Carl Zeiss, with an accelerating voltage of 1.5 kV and the use of an SE2 detector.

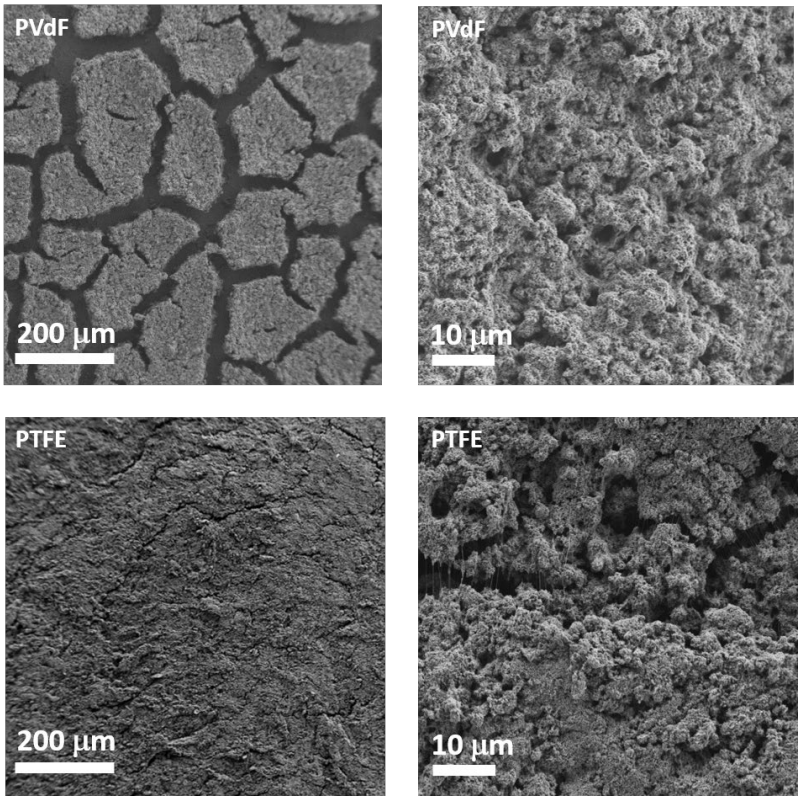

Figure S12. SEM images of PTFE and PVdF electrodes at different magnifications.

8. Carbon black contribution to the measured capacity

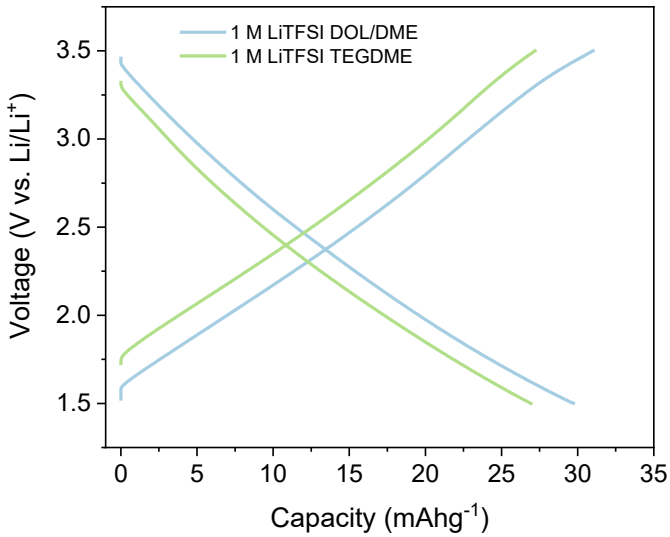

Figure S13. Printex XE2 charge/discharge profiles (electrodes with PTFE) in different electrolytes at current density of 5 mAg^{-1}.

Table S3. Measured capacities at 150 mA g^{-1} in 1 M LiTFSI DOL/DME and 1 M LiTFSI TEGDME obtained in 5th discharge ($C_{measured}$). Capacities after capacitance contribution subtraction (C_{real}). Capacity utilization calculated as C_{real} /$C_{theoretical}$.

	$C_{measured}$ (mAh g^{-1})	C_{real} (mAh g^{-1})	Utilization (%)
1 M LiTFSI DOL/DME	144	130	87%
1 M LiTFSI TEGDME	148	132	88%

9. Overpotentials in half-cell and symmetric cell

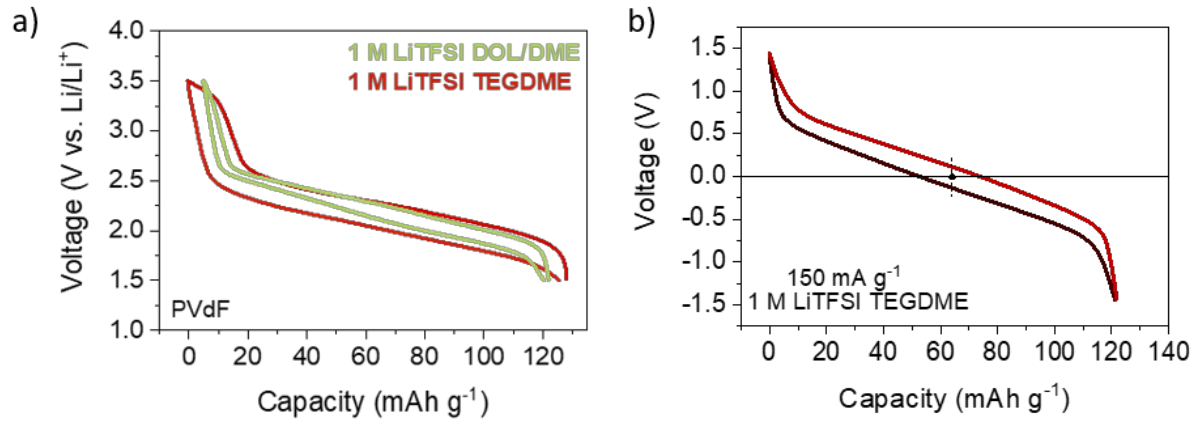

Figure S14. a) Voltage hysteresis of DAAQ-TFP-COF//Li half-cell in 1 M LiTFSI DOL/DME (green) and 1 M LiTFSI TEGDME (red). b) Voltage hysteresis of DAAQ (+)//DAAQ (-) symmetric cell in 1 M LiTFSI TEGDME.

DAAQ-TFP-COF overpotentials were obtained by dividing half-cell hysteresis by two and symmetric cell hysteresis by four (accounting for the presence of two organic electrodes).[25]

10. Rate capability performance in half-cell

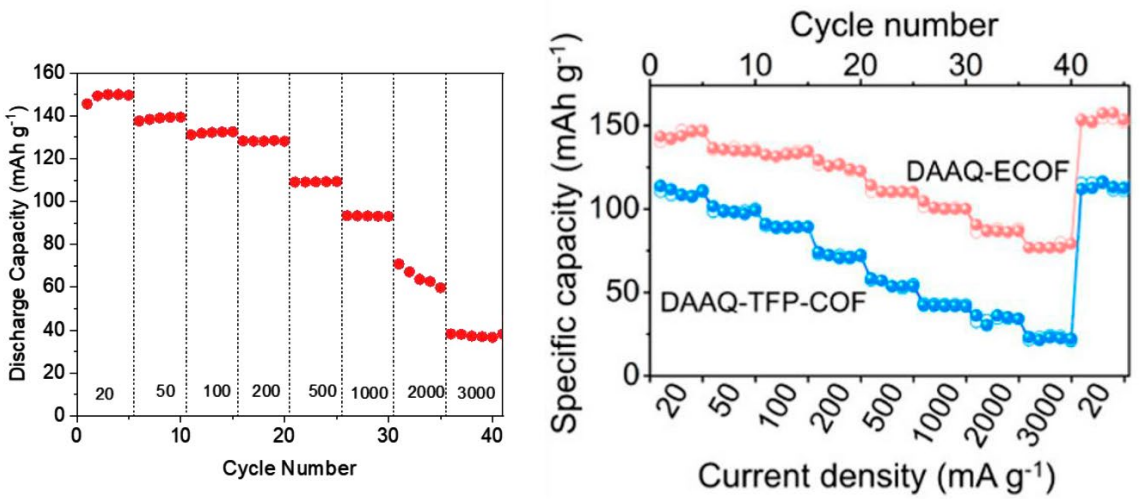

Figure S15. a) Rate capability performance of DAAQ-TFP-COF (in 1 M LiTFSI TEGDME electrolyte and TPFE as binder) and b) comparison with that of exfoliated DAAQ-TFP-COF (DAAQ-ECOF) in Li half-cell.[3]

11. *Ex-situ* infrared (IR) spectroscopy

Ex situ experiments were performed under an inert atmosphere using an ATR-IR Alpha II (Bruker) equipped with a Ge crystal. Measurements were collected and averaged over 64 scans in the range between 4000 and 500 cm^{-1} with a resolution of 4 cm^{-1}. Electrodes were harvested from Swagelok cells in 3rd charge or discharge (in 1 M LiTFSI TEGDME, at 150 mA g^{-1}). Cells were then transferred inside the glovebox and disassembled. Electrodes were washed three times in 2 ml of fresh DME to wash out any residual salt that would have an IR band, and dried overnight. All electrode handling and subsequent measurements were performed in an inert atmosphere, to prevent any sample degradation.

12. Evolution of galvanostatic charge/discharge profiles in Mg electrolytes

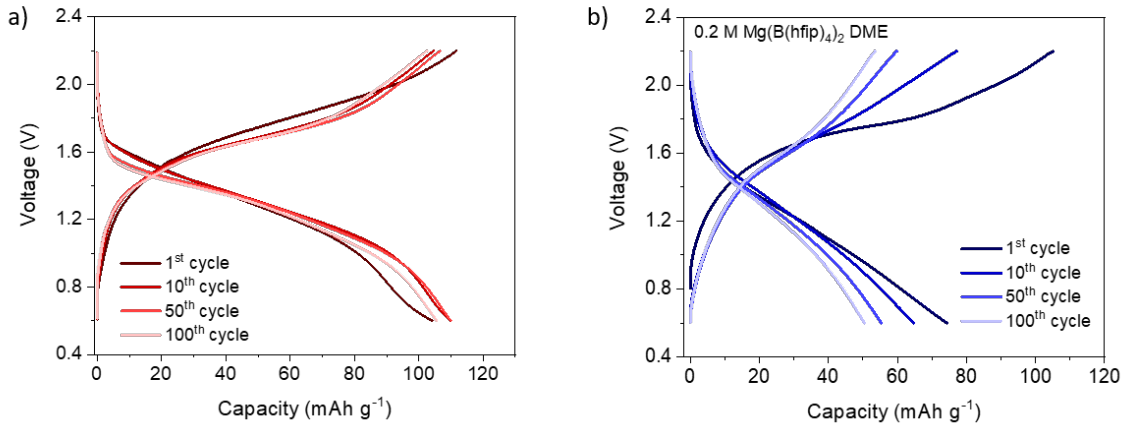

Figure S16. a) Evolution of DAAQ-TFP-COF voltage profile over 100 cycles in 0.6 M $MgCl_2$ – 1.2 M $MgCl_2$ DME. b) Evolution of DAAQ-TFP-COF voltage profile over 100 cycles in 0.2 M $Mg(B(hfip)_4)_2$ DME.

.

13. EDX elemental mapping

EDX mapping was performed on FE-SEM Supra 35 VP Carl Zeiss, at an accelerating voltage of 20 kV with the use of Oxford Instrument Ultim Max 100 EDX detector. Electrodes were prepared the same way as for infrared measurements. Samples were transferred in vacuum holder, to prevent sample degradation in ambient atmosphere.

Table S4. SEM/EDX of pristine DAAQ-TFP-COF electrode, electrode discharged in chloride-containing (red shade) and chloride-free (blue) Mg electrolyte.

	C	**O**	**F**	**Mg**	**Cl**
Pristine electrode	86.8	8.4	4.8	-	-
Discharged in **$Mg(TFSI)_2$-2MgCl2**	78.8	11.0	5.9	2.2	2.1
Discharged in **$Mg(B(hfip)_4)_2$**	77.6	11.6	9.4	1.4	-

In chloride-containing electrolyte, Mg/Cl ratio in discharged electrodes indicates coordination predominantly done with $MgCl^+$ cationic complex.

In chloride-free electrolyte, capacity utilization was lower than in the case of chloride-containing electrolyte (around 50%), which is reflected in lower overall Mg concentration. Concentration of F, present in pristine electrode as part of PTFE binder, increases in electrode discharged in chloride-free electrolyte. This, combined with the mass increase (mass of pristine electrode and electrode after discharge and washing) of around 30%, indicates partial contribution of bulky ionic complexes in coordination of reduced COF.

14. References

[1] *Sci. Rep.* **2015**, *5*, 8225.

[2] *J. Mater. Chem. A*, **2016**, *4*, 18621.

[3] *J. Am. Chem. Soc.* **2017**, *139*, 4258.

[4] *Angew. Chem. Int. Ed.* **2018**, *57*, 9443.

[5] *Angew. Chem. Int. Ed.* **2019**, *58*, 849.

[6] *Nanoscale*, **2019**, *11*, 5330.

[7] *Adv. Mater.* **2019**, *31*, 1901478.

[8] *ChemSusChem* **2019**, *13*, 2457.

[9] *J. Am. Chem. Soc.* **2020**, *142*, 16.

[10] *Angew. Chem. Int. Ed.* **2020**, *59*, 20385.

[11] *J. Mater. Chem. A*, **2021**, *9*, 10661.

[12] *Adv. Energy Mater.* **2021**, *11*, 2003735.

[13] *ACS Appl. Energy Mater.* **2021**, *4*, 350.

[14] *Adv. Funct. Mater.* **2021**, *31*, 1.

[15] *Energy Storage Mater.* **2021**, *36*, 347.

[16] *J. Am. Chem. Soc.* **2022**, *144*, 21, 9434.

[17] *Angew. Chem. Int. Ed.* **2022**, *61*, e202207043.

[18] *J. Energy Chem.* **2022**, *69*, 428.

[19] *Mater. Chem. Front.* **2022**, *6*, 2545.

[20] *Adv. Funct. Mater.* **2022**, *32*, 2107703.

[21] *Energy Storage Mater.* **2022**, *48*, 439.

[22] *J. Am. Chem. Soc.* **2023**, *145*, 2840.

[23] *J. Am. Chem. Soc.* **2023**, *145*, 1022.

[24] *J. Am. Chem. Soc.* **2013**, *135*, 16821–16824.

[25] *Batter. Supercaps* **2023**, *6* (2).